Acta Crystallographica Section C
Crystal Structure Communications
ISSN 0108-2701

Four differently substituted 2-aryl-2,3,4,5-tetrahydro-1*H*-1,4-epoxy-1-benzazepines: hydrogen-bonded structures in one, two and three dimensions

Sandra L. Gómez,[a] Carlos M. Sanabria,[a] Alirio Palma,[a] Ali Bahsas,[b] Justo Cobo[c] and Christopher Glidewell[d]*

[a]Laboratorio de Síntesis Orgánica, Escuela de Química, Universidad Industrial de Santander, AA 678 Bucaramanga, Colombia, [b]Laboratorio de RMN, Grupo de Productos Naturales, Departamento de Química, Universidad de los Andes, Mérida 5101, Venezuela, [c]Departamento de Química Inorgánica y Orgánica, Universidad de Jaén, 23071 Jaén, Spain, and [d]School of Chemistry, University of St Andrews, Fife KY16 9ST, Scotland
Correspondence e-mail: cg@st-andrews.ac.uk

Received 16 July 2009
Accepted 30 July 2009
Online 19 August 2009

In (2*RS*,4*SR*)-7-chloro-2-*exo*-(2-chloro-6-fluorophenyl)-2,3,4,5-tetrahydro-1*H*-1,4-epoxy-1-benzazepine, $C_{16}H_{12}Cl_2FNO$, (I), molecules are linked into chains by a single C—H···π(arene) hydrogen bond. (2*RS*,4*SR*)-2-*exo*-(2-Chloro-6-fluorophenyl)-2,3,4,5-tetrahydro-1*H*-1,4-epoxy-1-benzazepine, $C_{16}H_{13}ClFNO$, (II), is isomorphous with compound (I) but not strictly isostructural with it, as the hydrogen-bonded chains in (II) are linked into sheets by an aromatic π–π stacking interaction. The molecules of (2*RS*,4*SR*)-7-methyl-2-*exo*-(4-methylphenyl)-2,3,4,5-tetrahydro-1*H*-1,4-epoxy-1-benzazepine, $C_{18}H_{19}NO$, (III), are linked into sheets by a combination of C—H···N and C—H···π(arene) hydrogen bonds. (2*S*,4*R*)-2-*exo*-(2-Chlorophenyl)-2,3,4,5-tetrahydro-1*H*-1,4-epoxy-1-benzazepine, $C_{16}H_{14}ClNO$, (IV), crystallizes as a single enantiomer and the molecules are linked into a three-dimensional framework structure by a combination of one C—H···O hydrogen bond and three C—H···π(arene) hydrogen bonds.

Comment

We report here the structures of four new substituted 2-aryl-1,4-epoxytetrahydro-1-benzazepines, namely (2*RS*,4*SR*)-7-chloro-2-*exo*-(2-chloro-6-fluorophenyl)-2,3,4,5-tetrahydro-1*H*-1,4-epoxy-1-benzazepine, (I), (2*RS*,4*SR*)-2-*exo*-(2-chloro-6-fluorophenyl)-2,3,4,5-tetrahydro-1*H*-1,4-epoxy-1-benzazepine, (II), (2*RS*,4*SR*)-7-methyl-2-*exo*-(4-methylphenyl)-2,3,4,5-tetrahydro-1*H*-1,4-epoxy-1-benzazepine, (III), and (2*S*,4*R*)-2-*exo*-(2-chlorophenyl)-2,3,4,5-tetrahydro-1*H*-1,4-epoxy-1-benzazepine, (IV) (Fig. 1). The work reported here is a continuation of our structural study (Acosta *et al.*, 2008; Blanco *et al.*, 2008; Gómez *et al.*, 2008) of 2-substituted 1,4-epoxytetrahydro-1-benzazepines, which included two close analogues of the present compounds, namely compounds (V) and (VI). Compounds (I)–(IV) were all synthesized using our previously reported synthetic approach (Gómez Ayala *et al.*, 2006), with the eventual aim of identifying structurally novel antiparasitic compounds which are active against *Trypanosoma cruzi* and *Leishmania chagasi* parasites (Palma *et al.*, 2009).

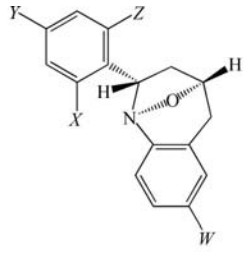

(I) W = Cl, X = Cl, Y = H, Z = F
(II) W = H, X = Cl, Y = H, Z = F
(III) W = Me, X = H, Y = Me, Z = H
(IV) W = H, X = H, Y = H, Z = Cl
(V) W = Cl, X = H, Y = Cl, Z = H
(VI) W = Cl, X = H, Y = H, Z = Cl
(VII) W = Me, X = Cl, Y = H, Z = H

Compounds (I)–(III) all crystallize as racemates, while the crystals of (IV) contain only a single enantiomer, *viz.* (2*S*,4*R*), in the crystal selected for data collection. Given the racemic nature of (I)–(III) and the absence of any reagent in the synthetic procedure likely to be able to provide enantiomeric selectivity, it seems probable that (IV) is, in fact, produced as a mixture of (2*S*,4*R*) and (2*R*,4S) enantiomers, but that it happens to crystallize as a conglomerate rather than as a racemate. In this connection, it is interesting to note that, while (V) crystallizes as a racemate in the space group $Pna2_1$, (VI) crystallizes as a single enantiomer in the space group $P2_12_12_1$ (Gómez *et al.*, 2008).

Compounds (I) and (II), which differ only in the presence of the 7-chloro substituent in (I), are isomorphous, with similar unit-cell dimensions and similar atomic coordinates for the corresponding atoms. However, they are not strictly isostructural (Acosta *et al.*, 2009), as the direction-specific intermolecular interactions in the two crystal structures are subtly different, as discussed below. Although pairs of analogous compounds carrying, respectively, a methyl or a chloro substituent at equivalent sites are not infrequently isomorphous, no such relationship is evident for (III) and (V), which crystallize, respectively, in the space groups $P2_1/n$ and $Pna2_1$ and which exhibit entirely different modes of supramolecular aggregation.

The ring-puckering parameters (Cremer & Pople, 1975) for (I)–(IV) are collected in Table 1, along with those for (V) and (VI) (Gómez *et al.*, 2008) for comparison. All six compounds exhibit very similar shapes for the fused heterocyclic ring system. The five-membered ring component in each of (I), (II), (V) and (VI) adopts a nearly perfect half-chair conformation, for which the idealized value of the puckering angle φ

 doi:10.1107/S0108270109030339

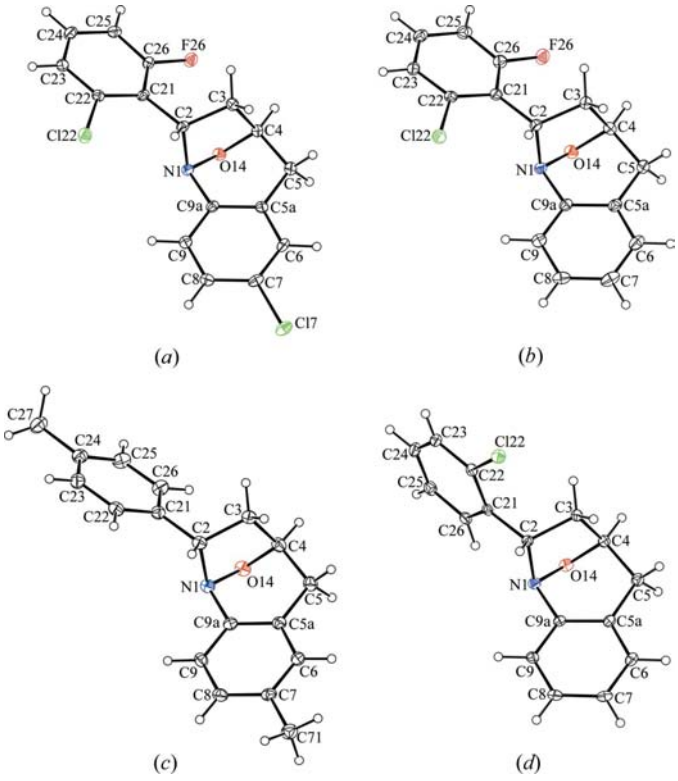

Figure 1
The molecular structures of (*a*) compound (I), (*b*) compound (II), (*c*) compound (III) and (*d*) compound (IV), shown as the (2*S*,4*R*) form in each case. Displacement ellipsoids are drawn at the 30% probability level.

is (36*k* + 18)°, where *k* represents an integer; the conformations in (III) and (IV) are intermediate between half-chair and envelope forms, for which the idealized value of φ is 36*k*°. The six-membered ring components all adopt conformations closer to the half-chair form, for which the ideal values of the ring-puckering angles are $\theta = 50.8°$ and $\varphi = (60k + 30)°$, than to the envelope conformation, where the ideal values of the puckering angles are $\theta = 54.7°$ and $\varphi = 60k°$.

The supramolecular aggregation in (I)–(IV) is dominated by C—H···O, C—H···N and C—H···π(arene) hydrogen bonds, augmented by aromatic π–π stacking interactions in (II) only. There are short intermolecular C—H···F contacts in (I) and (II) and an intermolecular C—H···Cl contact in (IV). None of these contacts is likely to be of structural significance, firstly because the C—H bonds involved are of low acidity, and secondly because it has been well established that F and Cl atoms when bound to C atoms are extremely poor acceptors of hydrogen bonds, even from donors such as O or N (Aakeröy *et al.*, 1999; Brammer *et al.*, 2001; Howard *et al.*, 1996; Thallapally & Nangia, 2001). Similarly, in the intermolecular C—H···N contacts in (I) and (II), involving a C—H bond of low acidity, the H···N distances are probably too long for these contacts to be of structural significance.

On this basis, the molecules of (I) are linked by just a single C—H···π(arene) hydrogen bond (Table 2) to form a simple chain running parallel to the [10$\bar{1}$] direction (Fig. 2), with no direction-specific interactions between adjacent chains. Entirely analogous chains are formed in (II), but these chains are now linked into sheets by a π–π stacking interaction. The fused aryl rings in the molecules at (*x*, *y*, *z*) and (1 − *x*, 1 − *y*, −*z*) are strictly parallel, with an interplanar spacing of 3.426 (2) Å, a ring-centroid separation of 3.810 (2) Å and a ring-centroid offset of 1.667 (2) Å. The effect of this interaction is to link the chains parallel to [10$\bar{1}$] into a sheet lying parallel to (101) (Fig. 3).

The crystal structure of (III) also contains sheets, but these are built solely from two hydrogen bonds, one each of the C—H···N and C—H···π(arene) types (Table 2). The C—H···π(arene) interaction links a pair of molecules into a cyclic centrosymmetric dimer centred at ($\frac{1}{2}$, 1, 0), and this dimer can be regarded as the building block for the sheet formation. The C—H···N hydrogen bond links the reference dimer centred at ($\frac{1}{2}$, 1, 0) directly to four other such dimers, *viz.* those centred at (0, $\frac{1}{2}$, $-\frac{1}{2}$), (0, $\frac{3}{2}$, $-\frac{1}{2}$), (1, $\frac{1}{2}$, $\frac{1}{2}$) and (1, $\frac{3}{2}$, $\frac{1}{2}$), and propagation of these two interactions then generates a hydrogen-bonded sheet lying parallel to (10$\bar{1}$) (Fig. 4).

Four hydrogen bonds, one of the C—H···O type and three of the C—H···π(arene) type, combine to link the molecules of (IV) into a single three-dimensional framework. The formation of the framework is most readily analysed in terms of two independent two-dimensional substructures. The three hydrogen bonds involving atoms C4, C6 and C8 as the donors combine to generate a sheet lying parallel to (001) (Fig. 5), while the two hydrogen bonds having C4 and C23 as the donors combine to form a sheet parallel to (100) (Fig. 6). The combination of the (100) and (001) sheets is sufficient to generate a three-dimensional structure.

It is of interest briefly to compare the aggregation in (I)–(IV) with that in the related compounds (V) and (VI) (Gómez *et al.*, 2008). In (V), the molecules are linked by a combination of C—H···O and C—H···N hydrogen bonds to form a chain of edge-fused $R_3^3(12)$ (Bernstein *et al.*, 1995) rings, while in (VI), a combination of two C—H···O hydrogen bonds and

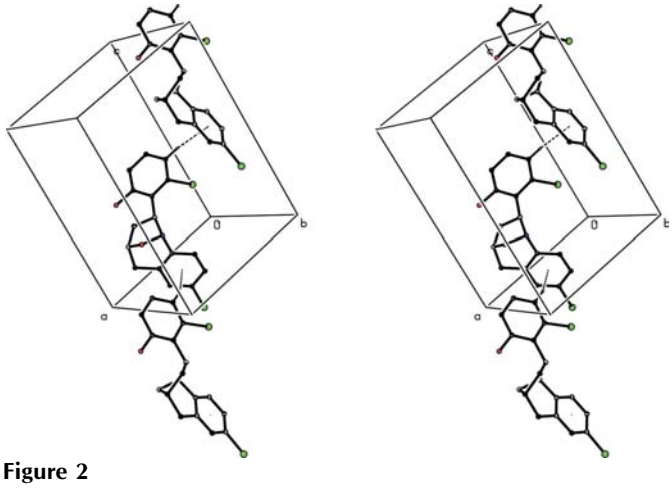

Figure 2
A stereoview of part of the crystal structure of (I), showing the formation of a hydrogen-bonded chain running parallel to the [10$\bar{1}$] direction. For the sake of clarity, H atoms not involved in the motif shown have been omitted.

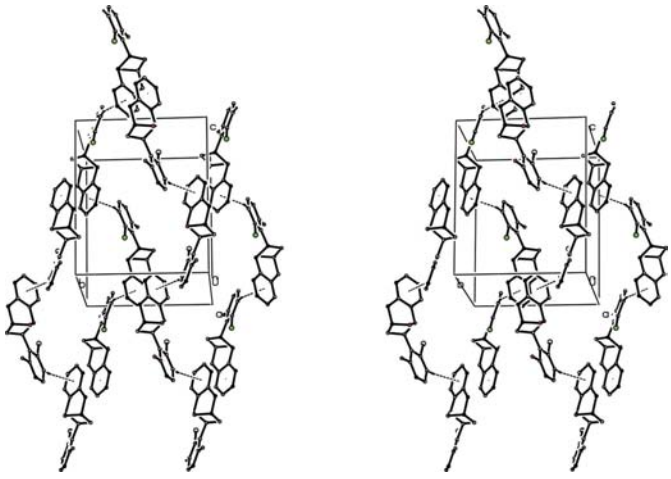

Figure 3
A stereoview of part of the crystal structure of (II), showing the formation of a sheet parallel to (101) built from the π-stacking of hydrogen-bonded chains parallel to [10$\bar{1}$]. For the sake of clarity, H atoms not involved in the motif shown have been omitted.

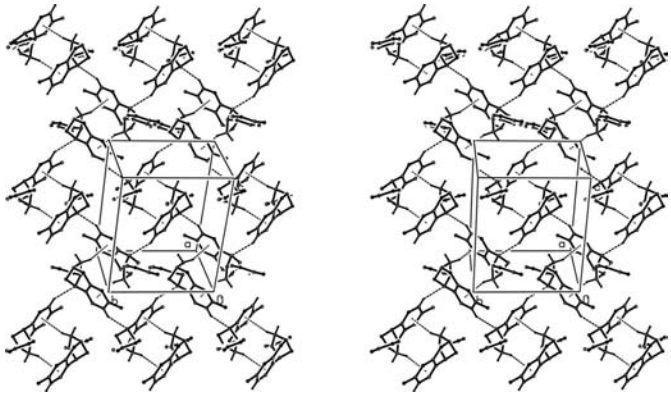

Figure 4
A stereoview of part of the crystal structure of (III), showing the formation of a hydrogen-bonded sheet parallel to (10$\bar{1}$) built from C—H···N and C—H···π(arene) hydrogen bonds. For the sake of clarity, H atoms bonded to C atoms that are not involved in the motifs shown have been omitted.

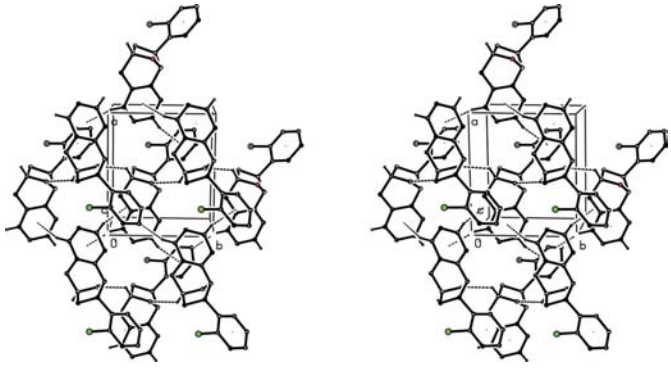

Figure 5
A stereoview of part of the crystal structure of (IV), showing the formation of a hydrogen-bonded sheet parallel to (001) built from one C—H···O and two C—H···π(arene) hydrogen bonds. For the sake of clarity, H atoms bonded to C atoms that are not involved in the motifs shown have been omitted.

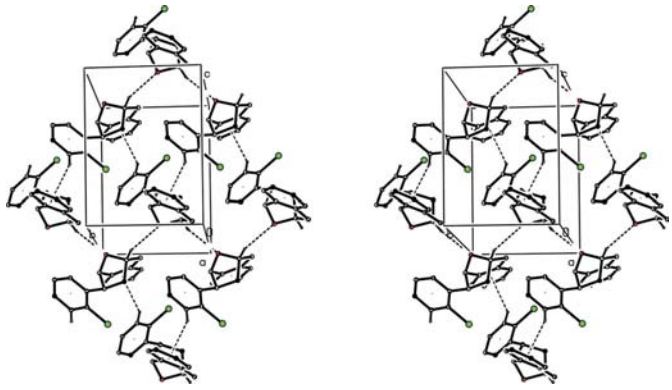

Figure 6
A stereoview of part of the crystal structure of (IV), showing the formation of a hydrogen-bonded sheet parallel to (100) built from one C—H···O and one C—H···π(arene) hydrogen bond. For the sake of clarity, H atoms bonded to C atoms that are not involved in the motifs shown have been omitted.

one C—H···π(arene) hydrogen bond generates a three-dimensional framework structure. In the course of the present work, we have also investigated (VII), which crystallizes in the space group $P\bar{1}$ with $Z' = 2$, but we have been unable to refine this below $R = 0.11$. However, it is clear that the two independent molecules within the asymmetric unit are linked by one C—H···O hydrogen bond and one C—H···N hydrogen bond to form an $R_2^2(8)$ motif, but that there are no further direction-specific interactions between the molecules. Thus, despite the very close constitutional, configurational and conformational similarity between the molecules of compounds (I)–(VII), no two of these compounds exhibits the same pattern of supramolecular aggregation.

Experimental

For the preparation of compounds (I)–(IV), sodium tungstate dihydrate, $Na_2WO_4{\cdot}2H_2O$ (10 mol%), followed by 30% aqueous hydrogen peroxide solution (added dropwise, 0.30 mol) were added to a stirred solution of the appropriately substituted 2-allyl-*N*-benzylaniline (0.10 mol) in methanol (34 ml) for (I), (III) and (IV), or in a mixture of methanol (34 ml) and nitromethane (3.4 ml) for (II). The resulting mixtures were then stirred at ambient temperature for periods ranging from 30 to 100 h. Each mixture was filtered and the solvent removed under reduced pressure. Toluene (40 ml) for compounds (I), (III) and (IV) or ethyl acetate (40 ml) for (II) was added to the solid residue and the resulting solution was heated to *ca* 353 K for periods ranging from 6 to 8 h. After cooling each solution to ambient temperature, the solvent was removed under reduced pressure and the crude products were purified by chromatography on silica gel using heptane–ethyl acetate (compositions ranged from 90:1 to 60:1 *v*/*v*) as eluant. Crystallization from heptane gave colourless crystals suitable for single-crystal X-ray diffraction. For (I), m.p. 429–430 K, yield 50%; MS (70 eV) *m*/*z* (%): 323 (M^+, ^{35}Cl, 17), 306 (3), 294 (1), 280 (1), 164 (3), 138 (100), 125 (6), 111 (4). For (II), m.p. 433–434 K, yield 65%; MS (70 eV) *m*/*z* (%): 289 (M^+, ^{35}Cl, 32), 272 (7), 260 (1), 246 (3), 130 (4), 104 (100), 91 (10), 77 (10). For (III), m.p. 374–376 K, yield 45%; MS (70 eV) *m*/*z* (%): 265 (M^+, 35), 248 (18), 222 (10), 207 (5), 146 (7), 132 (23), 118 (100), 103 (12), 91 (30), 77 (18), 65 (9), 51 (5). For (IV), m.p. 385–387 K, yield 63%; MS

(70 eV) *m*/*z* (%): 271 (M^+, ^{35}Cl, 50), 254 (19), 242 (2), 228 (2), 130 (4), 104 (100), 91 (25), 77 (26).

Compound (I)

Crystal data

$C_{16}H_{12}Cl_2FNO$
M_r = 324.17
Monoclinic, $P2_1/n$
a = 9.2907 (11) Å
b = 10.8720 (9) Å
c = 13.4523 (13) Å
β = 95.964 (8)°
V = 1351.4 (2) Å^3
Z = 4
Mo $K\alpha$ radiation
μ = 0.49 mm^{-1}
T = 120 K
0.35 × 0.06 × 0.06 mm

Data collection

Bruker–Nonius KappaCCD diffractometer
Absorption correction: multi-scan (*SADABS*; Sheldrick, 2003)
T_{min} = 0.868, T_{max} = 0.971
19650 measured reflections
3105 independent reflections
1774 reflections with $I > 2\sigma(I)$
R_{int} = 0.103

Refinement

$R[F^2 > 2\sigma(F^2)]$ = 0.049
$wR(F^2)$ = 0.121
S = 1.07
3105 reflections
190 parameters
H-atom parameters constrained
$\Delta\rho_{max}$ = 0.38 e Å^{-3}
$\Delta\rho_{min}$ = −0.44 e Å^{-3}

Compound (II)

Crystal data

$C_{16}H_{13}ClFNO$
M_r = 289.72
Monoclinic, $P2_1/n$
a = 9.0768 (13) Å
b = 10.9461 (9) Å
c = 12.9971 (18) Å
β = 99.768 (9)°
V = 1272.6 (3) Å^3
Z = 4
Mo $K\alpha$ radiation
μ = 0.31 mm^{-1}
T = 120 K
0.32 × 0.27 × 0.22 mm

Data collection

Bruker–Nonius KappaCCD diffractometer
Absorption correction: multi-scan (*SADABS*; Sheldrick, 2003)
T_{min} = 0.894, T_{max} = 0.936
18555 measured reflections
2918 independent reflections
2085 reflections with $I > 2\sigma(I)$
R_{int} = 0.055

Refinement

$R[F^2 > 2\sigma(F^2)]$ = 0.047
$wR(F^2)$ = 0.137
S = 1.04
2918 reflections
181 parameters
H-atom parameters constrained
$\Delta\rho_{max}$ = 0.29 e Å^{-3}
$\Delta\rho_{min}$ = −0.37 e Å^{-3}

Compound (III)

Crystal data

$C_{18}H_{19}NO$
M_r = 265.34
Monoclinic, $P2_1/n$
a = 9.7687 (9) Å
b = 10.3022 (17) Å
c = 14.239 (2) Å
β = 108.222 (10)°
V = 1361.1 (3) Å^3
Z = 4
Mo $K\alpha$ radiation
μ = 0.08 mm^{-1}
T = 120 K
0.33 × 0.27 × 0.12 mm

Data collection

Bruker–Nonius KappaCCD diffractometer
Absorption correction: multi-scan (*SADABS*; Sheldrick, 2003)
T_{min} = 0.962, T_{max} = 0.991
20555 measured reflections
3133 independent reflections
1788 reflections with $I > 2\sigma(I)$
R_{int} = 0.096

Refinement

$R[F^2 > 2\sigma(F^2)]$ = 0.063
$wR(F^2)$ = 0.135
S = 1.08
3133 reflections
183 parameters
H-atom parameters constrained
$\Delta\rho_{max}$ = 0.27 e Å^{-3}
$\Delta\rho_{min}$ = −0.26 e Å^{-3}

Compound (IV)

Crystal data

$C_{16}H_{14}ClNO$
M_r = 271.73
Monoclinic, $P2_1$
a = 8.8558 (19) Å
b = 7.3585 (13) Å
c = 9.9622 (18) Å
β = 101.622 (17)°
V = 635.9 (2) Å^3
Z = 2
Mo $K\alpha$ radiation
μ = 0.29 mm^{-1}
T = 120 K
0.25 × 0.15 × 0.07 mm

Data collection

Bruker–Nonius KappaCCD diffractometer
Absorption correction: multi-scan (*SADABS*; Sheldrick, 2003)
T_{min} = 0.919, T_{max} = 0.980
10226 measured reflections
2889 independent reflections
2400 reflections with $I > 2\sigma(I)$
R_{int} = 0.048

Refinement

$R[F^2 > 2\sigma(F^2)]$ = 0.038
$wR(F^2)$ = 0.078
S = 1.08
2889 reflections
172 parameters
1 restraint
H-atom parameters constrained
$\Delta\rho_{max}$ = 0.23 e Å^{-3}
$\Delta\rho_{min}$ = −0.22 e Å^{-3}
Absolute structure: Flack (1983), 1323 Bijvoet pairs
Flack parameter: 0.07 (6)

Table 1
Ring-puckering parameters (Å, °) for compounds (I)–(VI).

	Five-membered ring		Six-membered ring		
Compound	Q_2	φ_2	Q	θ	φ
(I)	0.436 (3)	198.2 (4)	0.623 (3)	52.9 (3)	346.3 (3)
(II)	0.438 (3)	199.3 (3)	0.621 (2)	52.0 (2)	346.2 (3)
(III)	0.433 (2)	189.2 (3)	0.606 (2)	49.1 (2)	347.6 (3)
(IV)	0.441 (2)	193.8 (3)	0.625 (2)	53.9 (2)	346.8 (2)
(V)[a]	0.447 (3)	197.4 (4)	0.618 (3)	51.0 (3)	341.9 (4)
(VI)[a]	0.436 (6)	195.7 (8)	0.620 (5)	51.3 (3)	344.5 (7)

Note: (*a*) data taken from Gómez *et al.* (2008); puckering parameters for five-membered rings are defined for the atom sequence O14—N1—C2—C3—C4 and those for six-membered rings are defined for the atom sequence O14—N1—C9a—C5a—C5—C4.

All H atoms were located in difference maps and then treated as riding atoms in geometrically idealized positions, with C—H distances of 0.95 (aromatic), 0.98 (CH_3), 0.99 (CH_2) or 1.00 Å (aliphatic CH), and with U_{iso}(H) = kU_{eq}(C), where k = 1.5 for the methyl groups, which were permitted to rotate but not to tilt, and k = 1.2 for all other H atoms. For (IV), the absolute configuration of the molecules in the crystal selected for data collection was established as (2*S*,4*R*) by means of the Flack (1983) *x* parameter of 0.07 (6) and the Hooft *y* parameter (Hooft *et al.*, 2008) of 0.03 (4). Accordingly, the configuration of the reference molecules in the racemic compounds (I)–(III) was set to be *S* at C2, and on this basis all three compounds have configuration *R* at C4 for the reference molecules, so that the overall configuration for each of (I)–(III) is (2*SR*,4*RS*).

For all compounds, data collection: *COLLECT* (Hooft, 1999); cell refinement: *DIRAX*/*LSQ* (Duisenberg *et al.*, 2000); data reduction: *EVALCCD* (Duisenberg *et al.*, 2003); program(s) used to solve structure: *SIR2004* (Burla *et al.*, 2005); program(s) used to refine structure: *SHELXL97* (Sheldrick, 2008); molecular graphics:

Table 2
Hydrogen bonds and short intermolecular contacts (Å, °) for compounds (I)–(IV).

*Cg*1 represents the centroid of the C5a/C6–C9/C9a ring and *Cg*2 represents the centroid of the C21–C26 ring.

Compound	D—H···A	D—H	H···A	D···A	D—H···A
(I)	C3—H3B···N1^{i}	0.99	2.72	3.617 (3)	151
	C4—H4···F26^{ii}	1.00	2.41	3.325 (3)	152
	C23—H23···$Cg1^{iii}$	0.95	2.51	3.359 (3)	149
(II)	C3—H3B···N1^{i}	0.99	2.62	3.417 (3)	137
	C4—H4···F26^{ii}	1.00	2.41	3.356 (3)	158
	C23—H23···$Cg1^{iii}$	0.95	2.49	3.324 (3)	147
(III)	C8—H8···N1^{iv}	0.95	2.52	3.395 (3)	153
	C3—H3B···$Cg1^{v}$	0.99	2.77	3.465 (3)	127
(IV)	C3—H3B···Cl22^{vi}	0.99	2.81	3.781 (3)	169
	C4—H4···O14^{vii}	1.00	2.53	3.344 (3)	138
	C6—H6···$Cg1^{viii}$	0.95	2.83	3.657 (2)	146
	C8—H8···$Cg2^{ix}$	0.95	2.65	3.571 (2)	163
	C23—H23···$Cg1^{x}$	0.95	2.68	3.415 (2)	134

Symmetry codes: (i) $-x+\frac{3}{2}, y-\frac{1}{2}, -z+\frac{1}{2}$; (ii) $-x+2, -y+1, -z+1$; (iii) $x-\frac{1}{2}, -y+\frac{3}{2}, z+\frac{1}{2}$; (iv) $-x+\frac{3}{2}, y+\frac{1}{2}, -z+\frac{1}{2}$; (v) $-x+1, -y+2, -z$; (vi) $-x+1, y-\frac{1}{2}, -z+1$; (vii) $-x+1, y-\frac{1}{2}, -z$; (viii) $-x, y-\frac{1}{2}, -z$; (ix) $x-1, y, z$; (x) $-x+1, y+\frac{1}{2}, -z+1$.

PLATON (Spek, 2009); software used to prepare material for publication: *SHELXL97* and *PLATON*.

The authors thank 'Servicios Técnicos de Investigación of Universidad de Jaén' and the staff for data collection. JC thanks the Consejería de Innovación, Ciencia y Empresa (Junta de Andalucía, Spain), the Universidad de Jaén (project reference UJA_07_16_33) and Ministerio de Ciencia e Innovación (project reference SAF2008-04685-C02-02) for financial support. AP, SLG and CMS thanks COLCIENCIAS for financial support (grant No. 1102-408-20563).

Supplementary data for this paper are available from the IUCr electronic archives (Reference: FA3200). Services for accessing these data are described at the back of the journal.

References

Aakeröy, C. B., Evans, T. A., Seddon, K. R. & Pálinkó, I. (1999). *New J. Chem.* pp. 145–152.
Acosta, L. M., Bahsas, A., Palma, A., Cobo, J., Hursthouse, M. B. & Glidewell, C. (2009). *Acta Cryst.* C**65**, o92–o96.
Acosta, L. M., Bahsas, A., Palma, A., Cobo, J., Low, J. N. & Glidewell, C. (2008). *Acta Cryst.* C**64**, o514–o518.
Bernstein, J., Davis, R. E., Shimoni, L. & Chang, N.-L. (1995). *Angew. Chem. Int. Ed. Engl.* **34**, 1555–1573.
Blanco, M. C., Raysth, W., Palma, A., Cobo, J., Low, J. N. & Glidewell, C. (2008). *Acta Cryst.* C**64**, o524–o528.
Brammer, L., Bruton, E. A. & Sherwood, P. (2001). *Cryst. Growth Des.* **1**, 277–290.
Burla, M. C., Caliandro, R., Camalli, M., Carrozzini, B., Cascarano, G. L., De Caro, L., Giacovazzo, C., Polidori, G. & Spagna, R. (2005). *J. Appl. Cryst.* **38**, 381–388.
Cremer, D. & Pople, J. A. (1975). *J. Am. Chem. Soc.* **97**, 1354–1358.
Duisenberg, A. J. M., Hooft, R. W. W., Schreurs, A. M. M. & Kroon, J. (2000). *J. Appl. Cryst.* **33**, 893–898.
Duisenberg, A. J. M., Kroon-Batenburg, L. M. J. & Schreurs, A. M. M. (2003). *J. Appl. Cryst.* **36**, 220–229.
Flack, H. D. (1983). *Acta Cryst.* A**39**, 876–881.
Gómez, S. L., Raysth, W., Palma, A., Cobo, J., Low, J. N. & Glidewell, C. (2008). *Acta Cryst.* C**64**, o519–o523.
Gómez Ayala, S. L., Stashenko, E., Palma, A., Bahsas, A. & Amaro-Luis, J. M. (2006). *Synlett*, pp. 2275–2277.
Hooft, R. W. W. (1999). *COLLECT*. Nonius BV, Delft, The Netherlands.
Hooft, R. W. W., Straver, L. H. & Spek, A. L. (2008). *J. Appl. Cryst.* **41**, 96–103.
Howard, J. A. K., Hoy, V. J., O'Hagan, D. & Smith, G. T. (1996). *Tetrahedron*, **52**, 12613–12622.
Palma, A., Yépes, A. F., Leal, S. M., Coronado, C. A. & Escobar, P. (2009). *Bioorg. Med. Chem. Lett.* **19**, 2360–2363.
Sheldrick, G. M. (2003). *SADABS*. Version 2.10. University of Göttingen, Germany.
Sheldrick, G. M. (2008). *Acta Cryst.* A**64**, 112–122.
Spek, A. L. (2009). *Acta Cryst.* D**65**, 148–155.
Thallapally, P. K. & Nangia, A. (2001). *CrystEngComm*, **27**, 1–6.